

Nonlinear Vibration Analysis of Functionally Graded Plate in Contact with Fluid: Analytical Study

S. Hashemi*
M.Sc. Student

A. A. Jafari†
Professor

In this paper, the nonlinear vibrations analysis of functionally graded (FG) rectangular plate in contact with fluid are investigated analytically using first order shear deformation theory (FSDT). The pressure exerted on the free surface of the plate by the fluid is calculated using the velocity potential function and the Bernoulli equation. With the aid of von Karman nonlinearity strain-displacement relations and Galerkin procedure the partial differential equations of motion are developed. The nonlinear equation of motion is then solved by modified Lindstedt-Poincare method. The effects of some system parameters such as vibration amplitude, fluid density, fluid depth ratio, volume fraction index and aspect ratio on the nonlinear natural frequency of the plate are discussed in detail.

Keywords: Nonlinear vibration; Functionally graded materials; Fluid pressure; First order shear deformation theory; modified Lindstedt-Poincare method

1 Introduction

Functionally graded materials (FGM) are a type of composite materials whose mechanical and thermal properties change from one surface to another according to a continuous function. The use of FGMs has increased significantly in recent decades. Due to its high thermal resistance and other properties, FGMs have many engineering applications in various industries such as defence industries and aerospace industries. FGMs are commonly used in the construction of equipment such as pressure vessels, turbine blades, heat exchangers, biomaterials like dental implants and etc. Plates are one of the most common FG structures which have many applications in the practical engineering. Therefore, due to their high importance, many studies have been reported on the dynamics of FG plates. Some researchers worked on the vibrations of FG plates based on classical plate theory (CPT). Zhang and Zhou [1] investigated free vibration, deflection and buckling analysis of the FG plates using the CPT based on physical neutral surface. Abrate [2] calculated natural frequencies of FG clamped and simply supported rectangular thin plates based on the CPT. Since rotatory inertia and shear deformation are neglected in the CPT, results given by CPT are admissible only for thin plates.

* M.Sc. Student, Faculty of Mechanical Engineering, K.N. Toosi University of Technology, Tehran, Iran
soheil.hashemi1994@gmail.com

† Corresponding Author, Professor, Department of Mechanical Engineering, K. N. Toosi University of Technology, Tehran, Iran AJafari@Kntu.ac.ir

Receive : 2019/07/13 Accepted : 2020/02/11

As a result, some researchers used first order shear deformation theory (FSDT) to take into account the effects of rotary inertia and shear deformation to analysis of thick plates [3-9]. Hosseini-Hashemi et al. [10] presented analytical method for analysis of free vibrations of FG rectangular plate on an elastic foundation using FSDT. By using element free kp-Ritz method, Zhao et al. [11] carried out the free vibrations of FG rectangular plate based on FSDT. They considered four types of FGM in their investigation. Yang and Shen [12] analyzed the free and forced vibrations of initially stressed FG plate in thermal environment with different boundary conditions on the basis of the FSDT. Gupta et al. [13] obtained linear frequencies of rectangular plate with different boundary constraint by using FSDT. During recent years, many studies have reported on the nonlinear analysis and large amplitude vibration. Some researchers has provided articles on the nonlinear vibrations of FG plates. Wang and Zu [14] presented a nonlinear vibrations analysis of FG plates incorporating the porosity. They used Almert's principle to derive the governing partial differential equations of plate and eventually solved it by Harmonic balance method. Yazdi [15] used the homotopy perturbation method to obtain nonlinear to linear frequency ratio of the FG rectangular plate. By using Fourier series, Woo et al. [16] investigated the effects of some parameters of the system on the dynamic behavior of FG plate. Malekzadeh and Monajjemzadeh [17] employed the CPT to analyze the nonlinear response of FG plates under moving load. Duc and Cong [18] used the Runge-Kutta method to determine the nonlinear dynamic response of an FG plate resting on elastic foundations that subjected to thermal, mechanical and damping loads. Fung and Chen [19] established nonlinear equations for an imperfect FG plate and then they considered effects of volume fraction index, geometric imperfection and initial stress on nonlinear vibrations. The finite element formulation, based on higher order shear deformation theory (HSDT), has been developed by Fakhari et al. [20] to analyze the nonlinear free and forced vibrations of FG plate with surface bonded piezoelectric layers in thermal environment. Hao et al. [21] dealt with the nonlinear dynamic analysis of FG cantilever plate under transversal excitation in thermal environment by using asymptotic perturbation method. They employed Runge-Kutta method and asymptotic perturbation method to obtain the nonlinear dynamic responses of the plate. An asymptotic perturbation method is used by Zhang et al. [22] to investigate the nonlinear responses of FG plate subjected to through the thickness thermal loading combined with external and parametric excitations. Based on HSDT, Duc et al. [23] presented an analysis of the nonlinear vibration of imperfect FG thick plates under blast and thermal load resting on the elastic foundations. A Very Large Floating Structure (VLFS) is a unique concept of sea structures, which may be constructed to create recreation parks, solar power plant, floating airport and etc. Flat floating structures are like a large plate which are on the surface of the water. These structures are very flexible in comparison to other floating structures and analysis of their elastic deformation is much more important than analysis of their rigid motion. Therefore, the hydrostatic analysis of these types of structures is one of the key stages in their design. For this purpose, a lot of studies have been done on the dynamics of plates in contact with fluid. When these structures are exposed to external fluid, some noise and vibration can be generated. Accordingly, Talebitooti et al. [24] presented an analytical model on sound transmission of the plate based on considering two-variable refined plate theory. The effect of hyperbolic shear deformation theory on the sound transmission loss (STL) of the infinite FG panels was inspected by Talebitooti et al. [25]. Talebitooti et al. [26] also proposed a theoretical model to opti mize STL as well as weight of the multilayered structure composed of double-walled shell interlayered with porous material based on Non-dominated sorting Genetic Algorithm. Motaharifar et al. [27] investigated the vibroacoustic behavior of a plate surrounded by a cavity containing an inclined part through surface crack with arbitrary position By using finite element method, Ugurlu et al. [28] investigated the influences of fluid and elastic foundation on the natural frequencies and associated mode shapes of the simply supported and clamped plate.

Kerboua et al. [29] studied vibration analysis of rectangular plates coupled with fluid based on Sanders' shell theory. A simple and effective procedure for determining the natural frequencies of rectangular bottom plate structures coupled with fluid is presented by Seung et al. [30]. Khorshidi and Farhadi [31] studied vibration analysis of a laminated composite rectangular plate in contact with a bounded fluid. They calculated frequencies of the plate coupled with sloshing fluid mode by using Rayleigh-Ritz method. Ergin and Ugurlu [32] investigated linear vibration analysis of cantilever plates partially submerged in fluid with the aid of finite element software. Shahbazzabar and Ranji [33] analyzed the influences of in-plane loads on vibration behavior of cross-ply laminated composite plates on elastic foundation and vertically in contact with fluid based on the FSDT. Khorshidi and Bakhsheshy [34] calculated the natural frequencies of FG rectangular plate in contact with a bounded fluid by use of Rayleigh-Ritz method. Shafiee et al. [35] presented a semi-analytical method to consider free vibrations of FG plate resting on Winkler elastic foundation and in contact with a quiescent fluid. Based on the Mindlin plate theory, Hosseini-Hashemi et al. [36] determined natural frequencies of rectangular plate, either immersed in fluid or floating on its free surface.

Shahbazzabar and Ranji [37] investigated the free vibration analysis of FG rectangular plates on two-parameter elastic foundation and vertically coupled with fluid based on the FSDT for different boundary conditions. Yousefzadeh et al. [38] investigated the effect of hydrostatic pressure on vibration of FG annular plate coupled with bounded fluid. Chang and Liu [39] studied the free and forced vibration analysis of composite plates in contact with fluid by ignoring the effects of rotatory inertia and transverse shear deformation. Wang and Yang [40] analyzed the nonlinear vibrations of moving FG plates containing porosities and contacting with liquid based on classical plate theory.

This paper present an analytical solution for nonlinear vibration analysis of functionally graded plate in contact with fluid based on FSDT. The pressure exerted on the free surface of the plate by the fluid is calculated using the velocity potential function and the Bernoulli equation. Within the framework of the developed model, von Karman nonlinearity strain-displacement relations and FSDT are used to obtain the partial differential equations of motion. By applying Galerkin method, the nonlinear partial differential equations of motion are transformed into the time-dependent nonlinear ordinary differential equations. The nonlinear equation of out of plane motion is then solved analytically by modified Lindstedt-Poincare method to obtain the nonlinear frequencies of the FG rectangular plate in contact with fluid. Finally, the effects of some system key parameters such as such as vibration amplitude, fluid density, fluid depth ratio, volume fraction index and aspect ratio on the nonlinear natural frequency of the plate in contact with fluid are discussed in detail. To validate the analysis, the results of this paper are compared with the published data and good agreements are found.

2 Geometry and properties of plate

Fig. (1) depicts an FGM plate composed of alumina and aluminium of length a , width b and thickness h which is in contact with fluid on one side. The plate simply supported on all four sides. The origin of the Cartesian coordinate system is located in the mid-plane of the FG plate. The distance from the mid-plane of the FG plate to the bottom rigid wall of the container is d . Mass density $\rho(z)$ and young's modulus $E(z)$ are assumed to vary continuously along the thickness of the plate according to power law distribution.

$$E(z) = (E_c - E_m) \left(\frac{2z + h}{2h} \right)^n + E_m \quad (1)$$

$$\rho(z) = (\rho_c - \rho_m) \left(\frac{2z + h}{2h} \right)^n + \rho_m \quad (2)$$

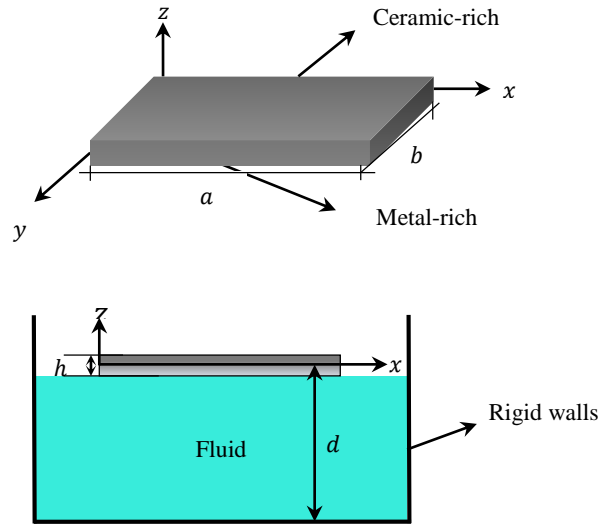


Figure 1 Geometry of an FG rectangular plate in contact with fluid

In which subscripts m and c denote bottom surface and top surface, respectively. Material properties used in the FG plate are listed in Table (1).

3 Equations of motion

The displacement field (u, v, w) of the FG plate according to the FSDT can be expressed as:

$$u(x, y, z, t) = u_0(x, y, t) + z\phi_x(x, y, t) \quad (3)$$

$$v(x, y, z, t) = v_0(x, y, t) + z\phi_y(x, y, t) \quad (4)$$

$$w(x, y, z, t) = w_0(x, y, t) \quad (5)$$

Where u_0, v_0 and w_0 are displacements of any point on the middle surface of the FG plate in the x, y and z directions, respectively. ϕ_x and ϕ_y are rotations about y and x axes, respectively. Assuming large deformations, the Von karman nonlinearity strain-displacement relations are given as follows:

$$\varepsilon_{xx} = \frac{\partial u_0}{\partial x} + \frac{1}{2} \left(\frac{\partial w_0}{\partial x} \right)^2 + z \frac{\partial \phi_x}{\partial x} \quad (6)$$

$$\varepsilon_{yy} = \frac{\partial v_0}{\partial y} + \frac{1}{2} \left(\frac{\partial w_0}{\partial y} \right)^2 + z \frac{\partial \phi_y}{\partial y} \quad (7)$$

$$\gamma_{xy} = \left(\frac{\partial u_0}{\partial y} + \frac{\partial v_0}{\partial x} + \frac{\partial w_0}{\partial x} \frac{\partial w_0}{\partial y} \right) + z \left(\frac{\partial \phi_x}{\partial y} + \frac{\partial \phi_y}{\partial x} \right) \quad (8)$$

$$\gamma_{xz} = \frac{\partial w_0}{\partial x} + \phi_x \quad (9)$$

$$\gamma_{yz} = \frac{\partial w_0}{\partial y} + \phi_y \quad (10)$$

Table 1 Material properties for FG plate

Properties	Ceramic (Al_2O_3)	Metal (Al)
Young's module	380 Gpa	70 Gpa
Density	$3800 \frac{kg}{m^3}$	$2702 \frac{kg}{m^3}$

Based on FSDT, the stress-strain relations are given by:

$$\begin{Bmatrix} \sigma_{xx} \\ \sigma_{yy} \\ \tau_{xy} \end{Bmatrix} = \begin{bmatrix} Q_{11} & Q_{12} & 0 \\ Q_{12} & Q_{22} & 0 \\ 0 & 0 & Q_{66} \end{bmatrix} \begin{Bmatrix} \varepsilon_{xx} \\ \varepsilon_{yy} \\ \gamma_{xy} \end{Bmatrix} \quad (11)$$

$$\begin{Bmatrix} \tau_{yz} \\ \tau_{xz} \end{Bmatrix} = \begin{bmatrix} Q_{44} & 0 \\ 0 & Q_{55} \end{bmatrix} \begin{Bmatrix} \gamma_{yz} \\ \gamma_{xz} \end{Bmatrix}$$

Where stiffness coefficients Q_{ij} are defined as:

$$Q_{11}(z) = Q_{22}(z) = \frac{E(z)}{1 - \nu(z)^2} \quad (12)$$

$$Q_{12}(z) = \frac{E(z)\nu(z)}{1 - \nu(z)^2} \quad (13)$$

$$Q_{44}(z) = Q_{55}(z) = Q_{66}(z) = \frac{E(z)}{2(1 + \nu(z))} \quad (14)$$

The Poisson ratio ν in the above relations is constant and equal to 0.3. On the basis of the FSDT, the motion equations of plate are [41]:

$$\frac{\partial N_{xx}}{\partial x} + \frac{\partial N_{xy}}{\partial y} = I_0 \frac{\partial^2 u_0}{\partial t^2} + I_1 \frac{\partial^2 \phi_x}{\partial t^2} \quad (15)$$

$$\frac{\partial N_{yy}}{\partial y} + \frac{\partial N_{xy}}{\partial x} = I_0 \frac{\partial^2 v_0}{\partial t^2} + I_1 \frac{\partial^2 \phi_y}{\partial t^2} \quad (16)$$

$$\frac{\partial Q_x}{\partial x} + \frac{\partial Q_y}{\partial y} + \mathcal{N}(w_0) + F(x, y, t) - \Delta P = I_0 \frac{\partial^2 w_0}{\partial t^2} \quad (17)$$

$$\frac{\partial M_{xx}}{\partial x} + \frac{\partial M_{xy}}{\partial y} - Q_x = I_1 \frac{\partial^2 u_0}{\partial t^2} + I_2 \frac{\partial^2 \phi_x}{\partial t^2} \quad (18)$$

$$\frac{\partial M_{yy}}{\partial y} + \frac{\partial M_{xy}}{\partial x} - Q_y = I_1 \frac{\partial^2 v_0}{\partial t^2} + I_2 \frac{\partial^2 \phi_y}{\partial t^2} \quad (19)$$

$\mathcal{N}(w_0)$ is:

$$\mathcal{N}(w_0) = \frac{\partial}{\partial x} \left(N_{xx} \frac{\partial w_0}{\partial x} + N_{xy} \frac{\partial w_0}{\partial y} \right) + \frac{\partial}{\partial y} \left(N_{yy} \frac{\partial w_0}{\partial y} + N_{xy} \frac{\partial w_0}{\partial x} \right) \quad (20)$$

N , M and Q are called the in-plane force resultants, moments resultants and transverse force resultants, I_0 , I_1 and I_2 are inertia related terms, ΔP is the total fluid pressure which is calculated in the next section, and F is the external load which is not considered in free vibrations.

In-plane inertia effects and rotary inertia effects can be ignored due to the thinness of the plate [42]. As a result, the Eqs. (15)-(19) reduce to:

$$\frac{\partial N_{xx}}{\partial x} + \frac{\partial N_{xy}}{\partial y} = 0 \quad (21)$$

$$\frac{\partial N_{yy}}{\partial y} + \frac{\partial N_{xy}}{\partial x} = 0 \quad (22)$$

$$\frac{\partial Q_x}{\partial x} + \frac{\partial Q_y}{\partial y} + \mathcal{N}(w_0) + F(x, y, t) - \Delta P = I_0 \frac{\partial^2 w_0}{\partial t^2} \quad (23)$$

$$\frac{\partial M_{xx}}{\partial x} + \frac{\partial M_{xy}}{\partial y} - Q_x = 0 \quad (24)$$

$$\frac{\partial M_{yy}}{\partial y} + \frac{\partial M_{xy}}{\partial x} - Q_y = 0 \quad (25)$$

The force and moment resultants of the FG plate can be written in terms of stress components across the thickness of the plate:

$$\begin{Bmatrix} N_{xx} \\ N_{yy} \\ N_{xy} \end{Bmatrix} = \int_{-\frac{h}{2}}^{+\frac{h}{2}} \begin{Bmatrix} \sigma_{xx} \\ \sigma_{yy} \\ \tau_{xy} \end{Bmatrix} dz \quad (26)$$

$$\begin{Bmatrix} M_{xx} \\ M_{yy} \\ M_{xy} \end{Bmatrix} = \int_{-\frac{h}{2}}^{+\frac{h}{2}} \begin{Bmatrix} \sigma_{xx} \\ \sigma_{yy} \\ \tau_{xy} \end{Bmatrix} z dz \quad (27)$$

Transverse force resultant and mass moments of inertia are:

$$\begin{Bmatrix} Q_x \\ Q_y \end{Bmatrix} = K \int_{-\frac{h}{2}}^{+\frac{h}{2}} \begin{Bmatrix} \tau_{xz} \\ \tau_{yz} \end{Bmatrix} dz \quad (28)$$

$$\begin{Bmatrix} I_0 \\ I_1 \\ I_2 \end{Bmatrix} = \int_{-\frac{h}{2}}^{+\frac{h}{2}} \begin{Bmatrix} 1 \\ z \\ z^2 \end{Bmatrix} \rho(z) dz \quad (29)$$

Where K is so-called transverse shear correction factor and is equal to 5/6.

4 Fluid formulation

In order to derive the mathematical formulations of fluid, it's assumed that the fluid is stationary, incompressible, irrotational and non-viscous. Also, the nonlinear effects of dynamic pressure at the fluid-plate interface are not considered. The motion of fluid is expressed by velocity potential function that satisfies the Laplace's equation throughout the whole fluid domain. This relation can be expressed in the Cartesian coordinate system as:

$$\nabla^2 \phi = \frac{\partial^2 \phi}{\partial x^2} + \frac{\partial^2 \phi}{\partial y^2} + \frac{\partial^2 \phi}{\partial z^2} = 0 \quad (30)$$

By using Bernoulli's equation, the fluid pressure at fluid-plate interface is given by:

$$P_L = P \left(z = -\frac{h}{2} \right) = -\rho_f \frac{\partial \phi}{\partial t} \left(z = -\frac{h}{2} \right) \quad (31)$$

Where ρ_f is fluid density per unit volume. Applied pressure on the upper surface of the plate is zero:

$$P_U = P \left(z = +\frac{h}{2} \right) = 0 \quad (32)$$

As a result, the total dynamics pressure on the FG plate along the z axis is as follows:

$$\Delta P = P_U - P_L \quad (33)$$

According to the method of separation of variables, velocity potential function takes the form:

$$\phi(x, y, z, t) = F(z) Q(x, y, t) \quad (34)$$

Where $F(z)$ and $Q(x, y, t)$ are two unknown functions to be determined later.

Because of the permanent contact between the peripheral fluid layer and the plate surface, the out-of-plane velocity component of the fluid on the plate surface should be the same as that of the plate. The compatibility condition of the plate surface can be expressed by:

$$\frac{\partial \phi}{\partial z} \left(z = -\frac{h}{2} \right) = \frac{\partial w}{\partial t} \quad (35)$$

By substituting Eq. (34) into Eq. (35) and then substituting $Q(x, y, t)$ in Eq. (34), velocity potential function at lower surface of the plate is given by:

$$\phi(x, y, z, t) = \frac{F(z)}{\frac{dF}{dz} \left(z = -\frac{h}{2} \right)} \frac{\partial w}{\partial t} \quad (36)$$

By inserting Eq. (36) into Eq. (30), second order differential equation is obtained as follows:

$$\frac{d^2 F(z)}{dz^2} - \mu_f^2 F(z) = 0 \quad (37)$$

Where μ_f is a plane wave number that is as follows [25]:

$$\mu_f = \pi \sqrt{\left(\frac{1}{a}\right)^2 + \left(\frac{1}{b}\right)^2} \quad (38)$$

The general solution of Eq. (37) is written as:

$$F(z) = A_1 e^{+\mu_f z} + A_2 e^{-\mu_f z} \quad (39)$$

A_1, A_2 in Eq. (39) are unknown coefficients to be determined later. By substituting Eq. (39) into Eq. (36), velocity potential function is obtained as:

$$\phi(x, y, z, t) = \frac{A_1 e^{+\mu_f z} + A_2 e^{-\mu_f z}}{\mu_f (A_1 e^{-\mu_f \frac{h}{2}} - A_2 e^{+\mu_f \frac{h}{2}})} \frac{\partial w}{\partial t} \quad (40)$$

The boundary constraint at the bottom of the tank, as shown in Fig. (1), represents rigid-wall condition and was referred to as the null-frequency condition, which is given by:

$$\frac{\partial \phi}{\partial z} (z = -d) = 0 \quad (41)$$

Substituting Eq. (40) into Eq. (41), velocity potential function is written as:

$$\phi(x, y, z, t) = \frac{e^{+\mu_f z + 2\mu_f d} + e^{-\mu_f z}}{\mu_f (e^{-\mu_f \frac{h}{2} + 2\mu_f d} - e^{+\mu_f \frac{h}{2}})} \frac{\partial w}{\partial t} \quad (42)$$

Substituting Eq. (42) into Eq. (31), the fluid pressure applying on the lower surface of the FG plate is found to be:

$$P_L = \frac{-\rho_f (e^{+2\mu_f d} + e^{+\mu_f h})}{\mu_f (e^{+2\mu_f d} - e^{+\mu_f h})} \frac{\partial^2 w}{\partial t^2} \quad (43)$$

As a result, by inserting Eq. (32) and (43) in Eq. (33), the total dynamics pressure on the FG plate can be obtained as:

$$\Delta P = P_U - P_L = \frac{\rho_f (e^{+2\mu_f d} + e^{+\mu_f h})}{\mu_f (e^{+2\mu_f d} - e^{+\mu_f h})} \frac{\partial^2 w}{\partial t^2} = M^* \frac{\partial^2 w}{\partial t^2} \quad (44)$$

By replacing Eq. (11) into Eq. (26)-(29) and substituting the results into the Eq. (21)-(25), equations of motion can be written in terms of displacements:

$$\begin{aligned} & A_{11} \left(\frac{\partial^2 u_0}{\partial x^2} + \frac{\partial w_0}{\partial x} \frac{\partial^2 w_0}{\partial x^2} \right) + B_{11} \frac{\partial^2 \phi_x}{\partial x^2} + A_{12} \left(\frac{\partial^2 v_0}{\partial x \partial y} + \frac{\partial w_0}{\partial y} \frac{\partial^2 w_0}{\partial x \partial y} \right) \\ & + B_{12} \left(\frac{\partial^2 \phi_y}{\partial x \partial y} \right) + A_{66} \left(\frac{\partial^2 u_0}{\partial y^2} + \frac{\partial^2 v_0}{\partial x \partial y} + \frac{\partial w_0}{\partial y} \frac{\partial^2 w_0}{\partial x \partial y} + \frac{\partial w_0}{\partial x} \frac{\partial^2 w_0}{\partial y^2} \right) \\ & + B_{66} \left(\frac{\partial^2 \phi_x}{\partial y^2} + \frac{\partial^2 \phi_y}{\partial x \partial y} \right) = 0 \end{aligned} \quad (45)$$

$$\begin{aligned} & A_{12} \left(\frac{\partial^2 u_0}{\partial x \partial y} + \frac{\partial w_0}{\partial x} \frac{\partial^2 w_0}{\partial x \partial y} \right) + B_{12} \frac{\partial^2 \phi_x}{\partial x \partial y} + A_{22} \left(\frac{\partial^2 v_0}{\partial y^2} + \frac{\partial w_0}{\partial y} \frac{\partial^2 w_0}{\partial y^2} \right) \\ & + B_{22} \left(\frac{\partial^2 \phi_y}{\partial y^2} \right) + A_{66} \left(\frac{\partial^2 u_0}{\partial x \partial y} + \frac{\partial^2 v_0}{\partial x^2} + \frac{\partial w_0}{\partial y} \frac{\partial^2 w_0}{\partial x^2} + \frac{\partial w_0}{\partial x} \frac{\partial^2 w_0}{\partial x \partial y} \right) \end{aligned} \quad (46)$$

$$\begin{aligned}
& +B_{66} \left(\frac{\partial^2 \phi_x}{\partial x \partial y} + \frac{\partial^2 \phi_y}{\partial x^2} \right) = 0 \\
KA_{55} \left(\frac{\partial^2 w_0}{\partial x^2} + \frac{\partial \phi_x}{\partial x} \right) & + KA_{44} \left(\frac{\partial^2 w_0}{\partial y^2} + \frac{\partial \phi_y}{\partial y} \right) + \frac{\partial w_0}{\partial x} \left(A_{11} \left(\frac{\partial^2 u_0}{\partial x^2} + \frac{\partial w_0}{\partial x} \frac{\partial^2 w_0}{\partial x^2} \right) \right. \\
& + B_{11} \frac{\partial^2 \phi_x}{\partial x^2} + A_{12} \left(\frac{\partial^2 v_0}{\partial x \partial y} + \frac{\partial w_0}{\partial y} \frac{\partial^2 w_0}{\partial x \partial y} \right) + B_{12} \left(\frac{\partial^2 \phi_y}{\partial x \partial y} \right) \\
& + 2 \frac{\partial^2 w_0}{\partial x \partial y} \left(A_{66} \left(\frac{\partial u_0}{\partial y} + \frac{\partial v_0}{\partial x} + \frac{\partial w_0}{\partial x} \frac{\partial w_0}{\partial y} \right) + B_{66} \left(\frac{\partial \phi_x}{\partial y} + \frac{\partial \phi_y}{\partial x} \right) \right) \\
& + \frac{\partial w_0}{\partial y} \left(A_{66} \left(\frac{\partial^2 u_0}{\partial x \partial y} + \frac{\partial^2 v_0}{\partial x^2} + \frac{\partial w_0}{\partial y} \frac{\partial^2 w_0}{\partial x^2} \right) \right) + B_{66} \left(\frac{\partial^2 \phi_x}{\partial x \partial y} + \frac{\partial^2 \phi_y}{\partial x^2} \right) \\
& + \frac{\partial w_0}{\partial x} \left(A_{66} \left(\frac{\partial^2 u_0}{\partial y^2} + \frac{\partial^2 v_0}{\partial x \partial y} + \frac{\partial w_0}{\partial y} \frac{\partial^2 w_0}{\partial x \partial y} + \frac{\partial w_0}{\partial x} \frac{\partial^2 w_0}{\partial y^2} \right) + B_{66} \left(\frac{\partial^2 \phi_x}{\partial y^2} + \frac{\partial^2 \phi_y}{\partial x \partial y} \right) \right) \\
& + \frac{\partial^2 w_0}{\partial y^2} \left(A_{12} \left(\frac{\partial u_0}{\partial x} + \frac{1}{2} \left(\frac{\partial w_0}{\partial x} \right)^2 \right) + B_{12} \frac{\partial \phi_x}{\partial x} \right. \\
& + \frac{\partial w_0}{\partial y} \left(A_{12} \left(\frac{\partial^2 u_0}{\partial x \partial y} + \frac{\partial w_0}{\partial x} \frac{\partial^2 w_0}{\partial x \partial y} \right) + B_{12} \frac{\partial^2 \phi_x}{\partial x \partial y} + A_{22} \left(\frac{\partial^2 v_0}{\partial y^2} + \frac{\partial w_0}{\partial y} \frac{\partial^2 w_0}{\partial y^2} \right) \right. \\
& \left. \left. + B_{22} \left(\frac{\partial^2 \phi_y}{\partial y^2} \right) \right) - \Delta P = I_0 \frac{\partial^2 w_0}{\partial t^2}
\end{aligned} \tag{47}$$

$$\begin{aligned}
& B_{11} \left(\frac{\partial^2 u_0}{\partial x^2} + \frac{\partial w_0}{\partial x} \frac{\partial^2 w_0}{\partial x^2} \right) + D_{11} \frac{\partial^2 \phi_x}{\partial x^2} + B_{12} \left(\frac{\partial^2 v_0}{\partial x \partial y} + \frac{\partial w_0}{\partial y} \frac{\partial^2 w_0}{\partial x \partial y} \right) \\
& + D_{12} \left(\frac{\partial^2 \phi_y}{\partial x \partial y} \right) + B_{66} \left(\frac{\partial^2 u_0}{\partial y^2} + \frac{\partial^2 v_0}{\partial x \partial y} + \frac{\partial w_0}{\partial y} \frac{\partial^2 w_0}{\partial x \partial y} + \frac{\partial w_0}{\partial x} \frac{\partial^2 w_0}{\partial y^2} \right) \\
& + D_{66} \left(\frac{\partial^2 \phi_x}{\partial y^2} + \frac{\partial^2 \phi_y}{\partial x \partial y} \right) - KA_{55} \left(\frac{\partial w_0}{\partial x} + \phi_x \right) = 0
\end{aligned} \tag{48}$$

$$\begin{aligned}
& B_{12} \left(\frac{\partial^2 u_0}{\partial x \partial y} + \frac{\partial w_0}{\partial x} \frac{\partial^2 w_0}{\partial x \partial y} \right) + D_{12} \frac{\partial^2 \phi_x}{\partial x \partial y} + B_{22} \left(\frac{\partial^2 v_0}{\partial y^2} + \frac{\partial w_0}{\partial y} \frac{\partial^2 w_0}{\partial y^2} \right) \\
& + D_{22} \left(\frac{\partial^2 \phi_y}{\partial y^2} \right) + B_{66} \left(\frac{\partial^2 u_0}{\partial x \partial y} + \frac{\partial^2 v_0}{\partial x^2} + \frac{\partial w_0}{\partial y} \frac{\partial^2 w_0}{\partial x^2} + \frac{\partial w_0}{\partial x} \frac{\partial^2 w_0}{\partial x \partial y} \right) \\
& + D_{66} \left(\frac{\partial^2 \phi_x}{\partial x \partial y} + \frac{\partial^2 \phi_y}{\partial x^2} \right) - KA_{44} \left(\frac{\partial w_0}{\partial y} + \phi_y \right) = 0
\end{aligned} \tag{49}$$

Where coefficients A_{ij} , B_{ij} and D_{ij} are called extensional stiffness, bending-extensional coupling stiffness and bending stiffness, respectively that are calculated from the following equation:

$$\begin{Bmatrix} A_{ij} \\ B_{ij} \\ D_{ij} \end{Bmatrix} = \int_{-\frac{h}{2}}^{+\frac{h}{2}} \begin{Bmatrix} 1 \\ z \\ z^2 \end{Bmatrix} Q_{ij}(z) dz, \quad i, j = 1, 2, 4, 5, 6 \tag{50}$$

The following boundary conditions for simply supported plate according to the FSDT are considered:

$$\text{at } x = 0, a \quad v_0 = w_0 = N_{xx} = M_{xx} = \phi_y = 0 \quad (51)$$

$$\text{at } y = 0, b \quad u_0 = w_0 = N_{yy} = M_{yy} = \phi_x = 0 \quad (52)$$

The boundary conditions in Eq. (51) and (52) are satisfied by the following admissible functions:

$$u_0(x, y, t) = \sum_{n=1}^{\infty} \sum_{m=1}^{\infty} U_{mn}(t) \cos(\alpha x) \sin(\beta y) \quad (53)$$

$$v_0(x, y, t) = \sum_{n=1}^{\infty} \sum_{m=1}^{\infty} V_{mn}(t) \sin(\alpha x) \cos(\beta y) \quad (54)$$

$$w_0(x, y, t) = \sum_{n=1}^{\infty} \sum_{m=1}^{\infty} W_{mn}(t) \sin(\alpha x) \sin(\beta y) \quad (55)$$

$$\phi_x(x, y, t) = \sum_{n=1}^{\infty} \sum_{m=1}^{\infty} X_{mn}(t) \cos(\alpha x) \sin(\beta y) \quad (56)$$

$$\phi_y(x, y, t) = \sum_{n=1}^{\infty} \sum_{m=1}^{\infty} Y_{mn}(t) \sin(\alpha x) \cos(\beta y) \quad (57)$$

Where $\alpha = \frac{n\pi}{a}$ and $\beta = \frac{m\pi}{b}$, and n and m are the half-wave numbers.

Considering only one term in the above series and by replacing Eq. (53)-(57) into Eq. (45)-(49) and then applying Galerkin procedure the time dependent nonlinear differential equations of motion can be derived after some mathematical simplifications as:

$$C_{11}W^2 - C_{12}U - C_{13}V - C_{14}X - C_{15}Y = 0 \quad (58)$$

$$C_{21}W^2 - C_{22}U - C_{23}V - C_{24}X - C_{25}Y = 0 \quad (59)$$

$$(I_0 + M^*) \ddot{W} + C_{31}W^3 + C_{32}W + C_{33}X + C_{34}Y - C_{35}UW - C_{36}VW - C_{37}XW - C_{38}YW = 0 \quad (60)$$

$$C_{41}W^2 - C_{42}W - C_{43}U - C_{44}V - C_{45}X - C_{46}Y = 0 \quad (61)$$

$$C_{51}W^2 - C_{52}W - C_{53}U - C_{54}V - C_{55}X - C_{56}Y = 0 \quad (62)$$

Where C_{ij} are coefficients that are related to the dimensions and plate properties and are presented in Appendix A. By substituting $U, V, X,$ and Y in terms of $W(t)$ obtained from the Eq. (58), (59), (61), and (62), into the Eq. (60) results in the nonlinear time-dependent equation in $W(t)$:

$$\frac{d^2W}{dt^2} + a_1 W + a_2 W^2 + a_3 W^3 = 0 \quad (63)$$

For the simplification, a set of dimensionless parameters are introduced as:

$$\tau = \frac{t}{h} \sqrt{\frac{E_m}{\rho_m}}, \quad \frac{W}{h} = \bar{W} \quad (64)$$

The non-dimensional form of Eq. (48) is obtained as:

$$\frac{d^2 \bar{W}}{d\tau^2} + \alpha \bar{W} + \beta \bar{W}^2 + \gamma \bar{W}^3 = 0 \quad (65)$$

Where the coefficients α, β and γ are given in Appendix B.

5 Solution method

In the present research, Modified Lindstedt-Poincare method is used to solve Eq. (65). The assumed initial condition is expressed as:

$$\bar{W}(0) = \frac{W_{max}}{h} = A \quad \frac{d\bar{W}(0)}{d\tau} = 0 \quad (66)$$

Where A is the non-dimensional maximum vibration amplitude. For the necessity of proposed method, a positive, dimensionless and small parameter must be defined. Therefore Eq. (65) should be rewritten as follows:

$$\ddot{\bar{W}} + \alpha \bar{W} + \epsilon \beta \bar{W}^2 + \epsilon \gamma \bar{W}^3 = 0 \quad (67)$$

Where ϵ is bookkeeping parameter that is defined as follows:

$$\epsilon = \frac{h}{a} \quad (68)$$

Linear frequency of FG plate from Eq. (67) is:

$$\alpha = \omega_l^2 \quad (69)$$

According to the References [43,44], $\bar{W}(\tau)$ and α can be written as a series in ϵ :

$$\bar{W} = \bar{W}_0 + \epsilon \bar{W}_1 + \epsilon^2 \bar{W}_2 + \dots \quad (70)$$

$$\alpha = \omega^2 + \epsilon c_1 + \epsilon^2 c_2 + \dots \quad (71)$$

Where ω and c_1, c_2, \dots and c_i (for $i = 1, \dots, \infty$) are unknown coefficients which are calculated in next section.

Substituting Eqs. (70) and (71) into Eq. (65), and equating the coefficients at ϵ^0, ϵ^1 and ϵ^2 to zero, yields the following equations:

$$\epsilon^0 : \quad \ddot{\bar{W}} + \omega^2 \bar{W}_0 = 0 \quad \bar{W}_0(0) = A \quad \frac{d\bar{W}_0}{d\tau}(0) = 0 \quad (72)$$

$$\epsilon^1 : \quad \ddot{\bar{W}}_1 + \omega^2 \bar{W}_1 = -c_1 \bar{W}_0 - \beta \bar{W}_0^2 - \gamma \bar{W}_0^3$$

$$\bar{W}_1(0) = 0 \quad \frac{d\bar{W}_1}{d\tau}(0) = 0 \quad (73)$$

$$\epsilon^2 : \quad \ddot{\bar{W}}_2 + \omega^2 \bar{W}_2 = -c_2 \bar{W}_0 - c_1 \bar{W}_1 - 2\beta \bar{W}_0 \bar{W}_1 - 3\gamma \bar{W}_1 \bar{W}_0^2$$

$$\bar{W}_2(0) = 0 \quad \frac{d\bar{W}_2}{d\tau}(0) = 0 \quad (74)$$

The result of solving Eq. (72) with the corresponding initial condition is as follow:

$$\bar{W}_0 = A \cos(\omega\tau) \quad (75)$$

Substituting Eq. (75) into Eq. (73) gives:

$$\ddot{\bar{W}}_1 + \omega^2 \bar{W}_1 = \left(-c_1 A - \frac{3}{4} \gamma A^3\right) \cos(\omega\tau) - \frac{1}{2} \beta A^2 \cos(2\omega\tau) \quad (76)$$

In order to have a periodic response for \bar{W}_1 , secular term must be eliminated in Eq. (76). So:

$$c_1 = -\frac{3}{4} \gamma A^2 \quad (77)$$

The solution of Eq. (76) is:

$$\bar{W}_1 = \left(\frac{\beta A^2}{3\omega^2} - \frac{\gamma A^3}{32\omega^2}\right) \cos(\omega\tau) + \frac{\beta A^2}{6\omega^2} \cos(2\omega\tau) + \frac{\gamma A^3}{32\omega^2} \cos(3\omega\tau) - \frac{\beta A^2}{2\omega^2} \quad (78)$$

Similarly, by substituting Eqs. (75) and (78) into Eq. (74) and avoiding the secular term, unknown coefficient c_2 is obtained:

$$c_2 = \frac{\beta \gamma A^3}{4\omega^2} - \frac{3\gamma^2 A^4}{128\omega^2} + \frac{5\beta^2 A^2}{6\omega^2} - \frac{3\beta \gamma A^3}{4\omega^2} + \frac{3\gamma^2 A^4}{64\omega^2} \quad (79)$$

Eq. (71), (77), and (79) give the nonlinear natural frequency, that is:

$$\omega_{NL} = \sqrt{\frac{\left(\alpha + \frac{3}{4} \gamma \epsilon A^2\right) + \sqrt{\left(\alpha + \frac{3}{4} \gamma \epsilon A^2\right)^2 + \left(2\beta \gamma A^3 - \frac{10\beta^2 A^2}{3} - \frac{3\gamma^2 A^4}{32}\right) \epsilon^2}}{2}} \quad (80)$$

After solving Eq. (74), \bar{W}_2 is obtained to be:

$$\begin{aligned} \bar{W}_2 = & \left(\frac{c_1 \beta A^2}{2\omega^4} - \frac{\beta^2 A^3}{3\omega^4} + \frac{21\beta \gamma A^4}{32\omega^4}\right) \\ & + \left(-\frac{5c_1 \beta A^2}{9\omega^4} - \frac{c_1 \gamma A^3}{256\omega^4} + \frac{61\beta^2 A^3}{144\omega^4} - \frac{17\beta \gamma A^4}{32\omega^4} \right. \\ & \left. - \frac{\gamma^2 A^5}{256\omega^4}\right) \cos(\omega\tau) + \left(\frac{c_1 \beta A^2}{18\omega^2} - \frac{\beta^2 A^3}{9\omega^2} - \frac{\beta \gamma A^4}{6\omega^2}\right) \cos(2\omega\tau) \\ & + \left(\frac{c_1 \gamma A^3}{256\omega^2} + \frac{\beta^2 A^3}{48\omega^2} + \frac{\beta \gamma A^4}{32\omega^2} + \frac{3\gamma^2 A^5}{1024\omega^2}\right) \cos(3\omega\tau) \\ & + \left(\frac{\beta \gamma A^4}{96\omega^2}\right) \cos(4\omega\tau) + \left(\frac{\gamma^2 A^5}{1024\omega^2}\right) \cos(5\omega\tau) \end{aligned} \quad (81)$$

Eventually, the second order approximation of the solution become as follows:

$$\bar{W}_{2nd} = \bar{W}_0 + \epsilon \bar{W}_1 + \epsilon^2 \bar{W}_2 \quad (82)$$

6 Comparison study

In this section, to examine the accuracy and efficiency of the present formulation, the results of this paper are compared with the existing data available in previously published papers.

As the first comparison study, taking linear parts of motion equations, the linear natural frequencies of the simply supported FG plate in vacuum can be obtained. Table (2) reported a comparison of the non-dimensional frequency parameter $\beta_L = \omega h \sqrt{\frac{\rho_c}{E_c}}$ for FG square plate obtained in this study with the results of existing literature. The material properties used in the plate are given in Table (1).

The exact solution given by Hosseini-Hashemi et al. [10] and element free kp-ritz method given by Zhao et al. [11] are also presented for direct comparison. As can be seen from Table (2), the present analysis gives highly precision results even for moderately thick plates.

The next study for verifying the results is devoted to the dimensionless frequencies parameters

$\gamma = \omega a^2 \sqrt{\frac{\rho h}{D}}$ of simply supported isotropic rectangular plate in contact with fluid are listed in

Table (3). The numerical results are performed for aspect ratio $\frac{a}{b} = 2$, length to thickness ratio $\frac{a}{h} = 20$ and thickness value $h = 0.1 m$. The exact closed form characteristics equation of this example is acquired by Hosseini-Hashemi et al. [32] based on the mindlin plate theory are added in Table (3). As seen in this table, noticeable difference between the results is only in higher mode shapes. The reason for this difference in higher mode shapes is neglecting of in plane inertia terms in the equations of motion.

As seen in the previous section, the nonlinear equation of transverse motion for FG rectangular plate in contact with fluid is solved by the modified Lindstedt-Poincare method. In order to ensure the accuracy and convergence of this solution approach, the nonlinear to linear frequency ratio of FG rectangular plate based on FSDT is obtained and then compared with the results given by Yazdi [15]. From Table (4), there is little difference between these two results. The reason for this difference is that the shear effects are ignored by Yazdi [15]. In other words, the results of the present study are more accurate than those by Yazdi [15].

Table 2 Comparison of fundamental frequency parameter $\beta = \omega h \sqrt{\frac{\rho_c}{E_c}}$ for Al/Al_2O_3 square plates

References	$\frac{a}{h}$	n				
		0	0.5	1	4	10
[10]		0.0148	0.0128	0.0115	0.0101	0.0096
[11]	20	0.0146	0.0124	0.0112	0.0097	0.0093
Present study		0.0148	0.0126	0.0113	0.0098	0.0094

[10]		0.0577	0.0492	0.0445	0.0383	0.0363
[11]	10	0.0567	0.0482	0.0435	0.0376	0.0359
Present study		0.0581	0.0494	0.0445	0.386	0.0369
[10]		0.2112	0.1806	0.1650	0.1371	0.1304
[11]	5	0.2055	0.1757	0.1587	0.1356	0.1284
Present study		0.2158	0.1847	0.1672	0.1435	0.1356

Table 3 Comparison of five frequency parameter for isotropic plate immersed in water.

References	$\frac{h_1}{a}$	Mode (m, n)				
		(1,1)	(2,1)	(3,1)	(1,2)	(2,2)
Hosseini-Hashemi et al. [36]	0	41.4293	64.5257	110.369	149.690	171.969
Present study		41.5627	68.8814	113.230	143.87	170.15
Hosseini-Hashemi et al. [36]	0.1	38.4638	59.9367	103.140	143.620	163.489
Present study		38.5686	64.1521	106.320	134.350	159.680
Hosseini-Hashemi et al. [36]	0.3	36.9582	57.1981	101.763	143.556	163.188
Present study		37.0557	63.0035	105.590	132.640	158.510
Hosseini-Hashemi et al. [36]	0.5	36.8523	56.9347	101.749	143.556	163.188
Present study		36.9502	62.9843	105.590	132.630	158.510
Hosseini-Hashemi et al. [36]	2.0	36.8455	56.9111	101.748	143.556	163.188
Present study		36.9297	62.9832	103.860	132.620	158.510
Hosseini-Hashemi et al. [36]	In vacuum	48.3006	76.3360	121.632	156.685	182.338
Present study		48.5006	76.8203	122.801	158.551	184.794

Table 4 Comparison of nonlinear to linear frequency ratio for square FGM plate ($\frac{a}{h} = 40$)

$\frac{W_{max}}{h}$	$n = 0.2$		$n = 10$	
	FSDT	CPT [15]	FSDT	CPT [15]
0.25	1.0529	1.0467	1.0473	1.0413
0.5	1.1962	1.1758	1.1766	1.1563
0.75	1.4005	1.3641	1.3630	1.3266
1.0	1.6428	1.5911	1.5860	1.5335
1.25	1.9086	1.8426	1.8323	1.7645
1.5	2.1895	2.1103	2.0937	2.0115
1.75	2.4805	2.3890	2.3654	2.2996
2	2.7785	2.6755	2.6442	2.5355

7 Results and discussion

In this section, the influences of some key plate parameters such as dimensionless vibration amplitude, aspect ratio, fluid density, depth fluid ratio and volume fraction index on the nonlinear frequency of FG rectangular plate in contact with fluid are presented in tabular and graphical forms. The results are reported for plate which is made of a mixture of aluminum (*Al*) and alumina (Al_2O_3) in which their material properties are listed in Table (1).

Table (5) provided the effects of dimensionless vibration amplitude on the nonlinear frequency parameter $\beta_{NL} = \omega_{NL} h \sqrt{\frac{\rho_m}{E_m}}$ for FG rectangular plate in vacuum and in contact with fluid for different volume fraction index. The numerical results are performed for aspect ratio $\frac{a}{b} = 5$ and length to thickness ratio $\frac{a}{h} = 20$. This table shows that the nonlinear frequency parameter β_{NL} increases by increasing the dimensionless vibrations amplitude for different volume fraction index. It is also seen from this table that when the plate is in contact with fluid, the nonlinear frequency parameter β_{NL} of FG plate takes lower values.

Table 5 nonlinear frequency parameter $\beta_{NL} = \omega_{NL} h \sqrt{\frac{\rho_m}{E_m}}$ for FG rectangular plate in vacuum and in contact with fluid
($\frac{a}{h} = 20$, $\frac{a}{b} = 5$)

	A	n				
		0	2	5	10	100
Plate in vacuum	0.25	0.3927	0.2798	0.2574	0.2444	0.2088
	0.5	0.4965	0.3610	0.3243	0.3035	0.2617
	0.75	0.6314	0.4649	0.4115	0.3814	0.3308
	1	0.7814	0.5796	0.5087	0.4688	0.4081
	1.5	1.1023	0.8230	0.7167	0.6570	0.5740
	2	1.4356	1.0748	0.9329	0.8533	0.7465
Plate in contact with fluid	0.25	0.3407	0.2359	0.2150	0.2033	0.1728
	0.5	0.4308	0.3044	0.2709	0.2524	0.2165
	0.75	0.5478	0.3920	0.3438	0.3172	0.2738
	1	0.6780	0.4886	0.4250	0.3899	0.3378
	1.5	0.9564	0.6938	0.5988	0.5465	0.4750
	2	1.2455	0.9061	0.7794	0.7097	0.6177

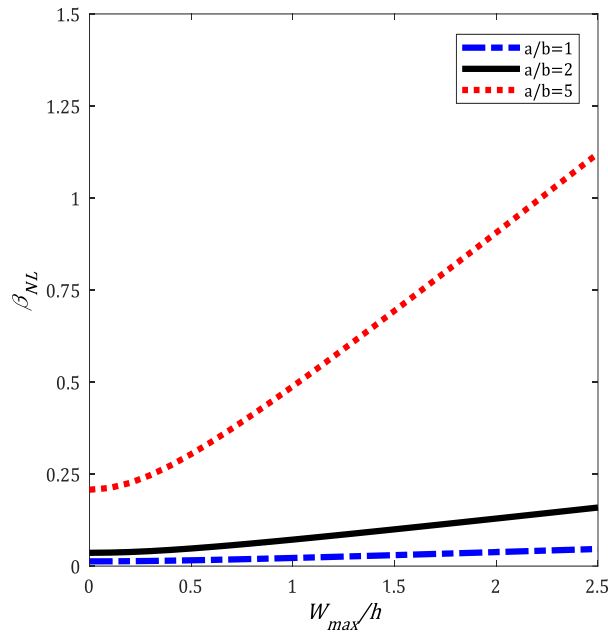


Figure 2 Effect of dimensionless vibration amplitude on nonlinear frequency parameter β_{NL} for different values of aspect ratio for ($n = 1$)

Figure (2) exhibits effect of dimensionless vibration amplitude $\frac{W_{max}}{h}$ on nonlinear frequency parameter β_{NL} of FG rectangular plate in contact with fluid for different values of aspect ratio when $n = 1$. It is seen from this figure, aspect ratios has noticeable effect on the nonlinear frequency parameter and by increasing the dimensionless vibrations amplitude the nonlinear frequency parameter increases. However, the slope of increase at $\frac{a}{b} = 5$ is higher.

In Figure (3), the variation of the nonlinear frequency parameter β_{NL} against the volume fraction index n for the simply supported FG rectangular plate is shown for different aspect ratio and $\frac{W_{max}}{h} = 1$. As is clear from this figure, that with the increase of the volume fraction index n , the nonlinear frequency parameter β generally decreased for any aspect ratio $\frac{a}{b}$.

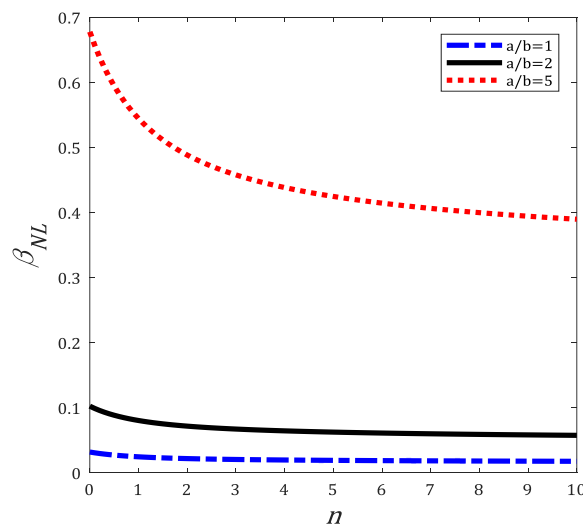


Figure 3 Variation of nonlinear frequency parameter β_{NL} versus the values of n for different aspect ratio ($\frac{W_{max}}{h} = 1$)

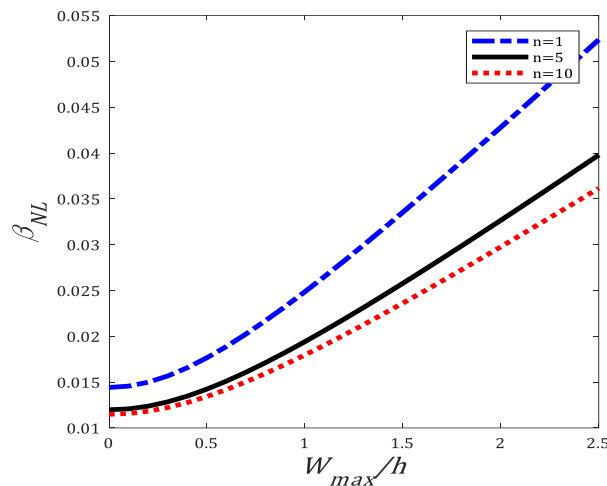


Figure 4 Variation of nonlinear frequency parameter β_{NL} versus dimensionless vibration amplitude for different values of n ($\frac{a}{b} = 1$)

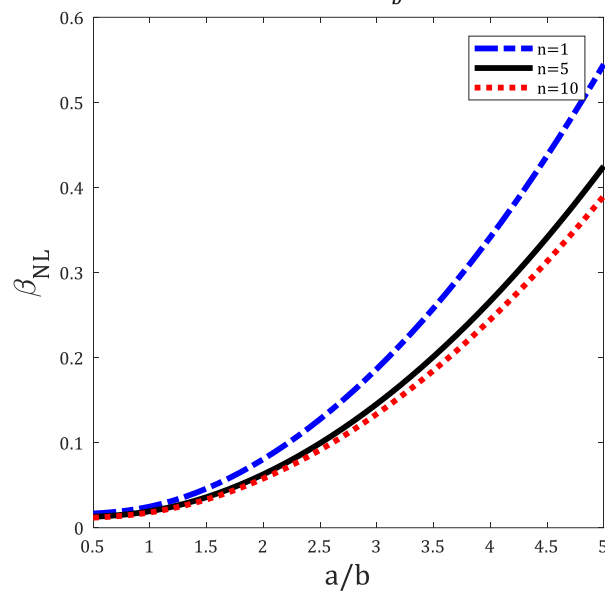


Figure 5 Aspect ratio effect on the nonlinear frequency parameter β_{NL} for different values of n ($\frac{W_{max}}{h} = 1$)

Figure (4) shows the behavior of the nonlinear frequency parameter β_{NL} versus the dimensionless vibration amplitude $\frac{W_{max}}{h}$ for the simply supported FG rectangular plate in contact with fluid for different values of volume fraction index n when $\frac{a}{b} = 1$. It is obvious that nonlinear frequency parameter β_{NL} increases as the dimensionless vibration amplitude $\frac{W_{max}}{h}$ increases.

Figure (5) displays the variation of the nonlinear frequency parameter β_{NL} against the aspect ratio $\frac{a}{b}$ for the simply supported FG rectangular plate in contact with fluid for different values of volume fraction index n when $\frac{W_{max}}{h} = 1$. It can apparently be observed that the nonlinear frequency parameter β_{NL} increases when the aspect ratio $\frac{a}{b}$ increases.

Figure (6) contains the plot of the nonlinear frequency parameter β_{NL} versus the dimensionless vibration amplitude $\frac{W_{max}}{h}$ for the simply supported FG rectangular plate in contact with fluid

with five different fluid when $\frac{a}{h} = 20$, $\frac{a}{b} = 2$ and $n = 10$. It is obviously seen from Figure 6 that the enhancement of the dimensionless vibration amplitude $\frac{W_{max}}{h}$, the nonlinear frequency parameter β_{NL} increases for any fluid density ρ . On the other hand, increasing the value of density ρ results the reduction of nonlinear frequency parameter β_{NL} .

Figure (7) demonstrates the effect of the depth fluid ratio $\frac{d}{h}$ on nonlinear frequency parameter β_{NL} for three different volume fraction index when $\frac{a}{h} = 20$, $\frac{a}{b} = 2$ and $\frac{W_{max}}{h} = 1$. It can be concluded from Figure (7) that by increasing the depth fluid ratio $\frac{d}{h}$, the nonlinear frequency parameter β_{NL} is increased, while for higher values of the non-dimensional depth of fluid $\frac{d}{h}$, the results convergent to specific value, which can also be reflected in Figure (7).

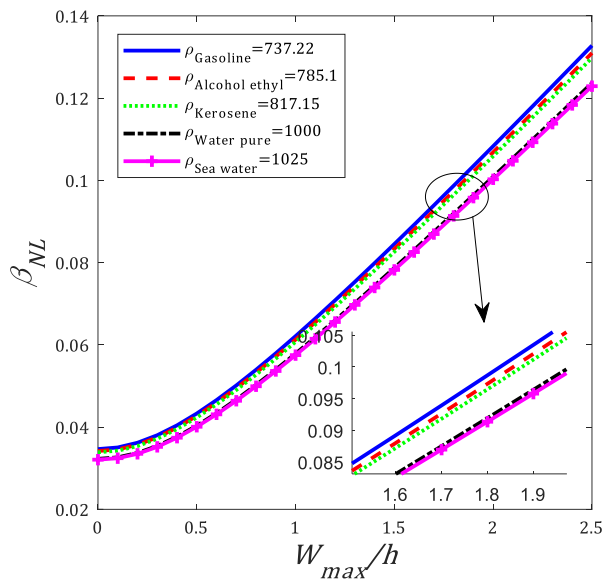


Figure 6 the nonlinear frequency parameter β_{NL} versus dimensionless vibration amplitude with five different fluid

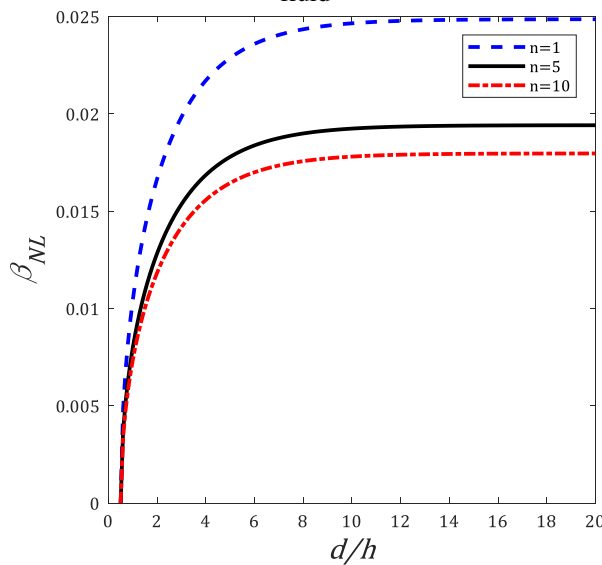


Figure 7 Effect of depth of the fluid on nonlinear frequency parameter β_{NL} for different values of n

8 Conclusion

In this study, the nonlinear free vibrations analysis of functionally graded (FG) rectangular plate which simply supported all edges and is in contact with fluid were investigated analytically. The material properties were assumed to be graded through the direction of plate thickness according to power law distribution. The pressure exerted on the free surface of the plate by the fluid is calculated using the velocity potential function and the Bernoulli equation. With the aid of von Karman nonlinearity strain-displacement relations, the partial differential equations of motion were developed based on FSDT. The nonlinear partial differential equations of motion were transformed into the time-dependent nonlinear ordinary differential equations by applying Galerkin procedure. The nonlinear equation of out of plane motion was then solved analytically by modified Lindstedt-Poincare method to determine the nonlinear frequencies of the FG rectangular plate in contact with fluid. The effects of some system parameters such as vibration amplitude, fluid density, fluid depth ratio, volume fraction index and aspect ratio on the nonlinear natural frequency of the plate were discussed in detail. To validate the analysis, the results of this paper were compared with the published data and good agreements were found.

References

- [1] Zhang, D.G., and Zhou, Y.H., "A Theoretical Analysis of FGM Thin Plates Based on Physical Neutral Surface", *Comp. Mater. Sci.* Vol. 44, pp. 716–720, (2008).
- [2] Abrate, S., "Functionally Graded Plates Behave Like Homogeneous Plates", *Compos. Part B-Eng.* Vol. 39, pp. 151–158, (2008).
- [3] Nguyen, T.K., Sab, K., and Bonnet, G., "First-order Shear Deformation Plate or Functionally Graded Materials", *Compos. Struct.* Vol. 83, pp. 25–36, (2008).
- [4] Timoshenko, S.P., "On the Transverse Vibrations of Bars of Uniform Cross-section", *Philos. Mag.* Vol. 43, pp. 125–131, (1922).
- [5] Ferreira, A.J.M., Batra, R.C., Roque, C.M.C., Qian, L.F., and Jorge, R.M.N., "Natural Frequencies of Functionally Graded Plates by a Meshless Method", *Compos. Struct.* Vol. 75, pp. 593–600, (2006).
- [6] Efraim, E., and Eisenberger, M., "Exact Vibration Analysis of Variable Thickness Thick Annular Isotropic and FGM Plates", *J. Sound Vib.* Vol. 299, pp. 720–738, (2007).
- [7] Zhao, X., Lee, Y.Y., and Liew, K.M., "Free Vibration Analysis of Functionally Graded Plates using the Element-free Kp-Ritz Method", *J. Sound Vib.* Vol. 319, pp. 918–939, (2009).
- [8] Abrate, S., "Free Vibration, Buckling, and Static Deflections of Functionally Graded Plates", *Compos. Sci. Technol.* Vol. 66, pp. 2383–2394, (2006).
- [9] Rani, R., and Lal, R., "Free Vibrations of Composite Sandwich Plates by Chebyshev Collocation Technique", *Composites Part B: Engineering*, Vol. 165, pp. 442–455, (2019).

- [10] Hosseini-Hashemi, S., Taher, H.R., Akhavan, H., Omid, M., “Free Vibration of Functionally Graded Rectangular Plates using First-order Shear Deformation Plate Theory”, *Applied Mathematical Modelling*, Vol. 34, pp. 1276–1291, (2010).
- [11] Zhao, X., Lee, Y.Y., and Liew, K.M., “Free Vibration Analysis of Functionally Graded Plates using the Element-free Kp-Ritz Method”, *Journal of Sound and Vibration*, Vol. 319, pp. 918–939, (2009).
- [12] Yang, J., and Shen, H.S., “Vibration Characteristics and Transient Response of Shear-deformable Functionally Graded Plates in Thermal Environments”, *Journal of Sound and Vibration*, Vol. 255, pp. 579–602, (2002).
- [13] Gupta, A., Talha, M., and Singh, B.N., “Vibration Characteristics of Functionally Graded Material Plate with Various Boundary Constraints using Higher Order Shear Deformation Theory”, *Composites Part B: Engineering*, Vol. 94, pp. 64–74, (2016).
- [14] Wang, Y.Q., and Zu, J.W., “Large-amplitude Vibration of Sigmoid Functionally Graded Thin Plates with Porosities”, *Thin-Walled Structures*, Vol. 119, pp. 911–924, (2017).
- [15] Yazdi, A.A., “Homotopy Perturbation Method for Nonlinear Vibration Analysis of Functionally Graded Plate”, *Journal of Vibration and Acoustics*, Vol. 135, pp. 12–21, (2013).
- [16] Woo, J., Meguid, S.A., and Ong, L.S., “Nonlinear Free Vibration Behavior of Functionally Graded Plates”, *Journal of Sound and Vibration*, Vol. 289, pp. 595–611, (2006).
- [17] Malekzadeh, P., and Monajjemzadeh, S.M., “Nonlinear Response of Functionally Graded Plates under Moving Load”, *Thin-Walled Structures*, Vol. 96, pp. 120–129, (2015).
- [18] Duc, N.D., and Cong, P.H., “Nonlinear Vibration of Thick FGM Plates on Elastic Foundation Subjected to Thermal and Mechanical Loads using the First-order Shear Deformation Plate Theory”, *Cogent Engineering*, Vol. 2, pp. 1045222, (2015).
- [19] Fung, C.P., and Chen, C.S., “Imperfection Sensitivity in the Nonlinear Vibration of Functionally Graded Plates”, *European Journal of Mechanics-A/Solids*, Vol. 25, pp. 425–461, (2006).
- [20] Fakhari, V., Ohadi, A., and Yousefian, P., “Nonlinear Free and Forced Vibration Behaviour of Functionally Graded Plate with Piezoelectric Layers in Thermal Environment”, *Composite Structures*, Vol. 93, pp. 2310–2321, (2011).
- [21] Hao, Y.X., Zhang, W., and Yang, J., “Nonlinear Oscillation of a Cantilever FGM Rectangular Plate Based on Third-order Plate Theory and Asymptotic Perturbation Method”, *Composites Part B: Engineering*, Vol. 42, pp. 402–415, (2011).
- [22] Zhang, W., Hao, Y., Guo, X., and Chen, L., “Complicated Nonlinear Responses of a Simply Supported FGM Rectangular Plate under Combined Parametric and External Excitations”, *Meccanica*, Vol. 47, pp. 985–1014, (2012).

- [23] Dinh Duc, N., Tuan, N.D., Tran, P., and Quan, T.Q., "Nonlinear Dynamic Response and Vibration of Imperfect Shear Deformable Functionally Graded Plates Subjected to Blast and Thermal Loads", *Mechanics of Advanced Materials and Structures*, Vol. 24, pp. 318-347, (2017).
- [24] Talebitooti, R., Johari, V., and Zarastvand, M., "Wave Transmission Across Laminated Composite Plate in the Subsonic Flow Investigating Two-variable Refined Plate Theory", *Latin American Journal of Solids and Structures*, Vol. 15, No. 5, (2018).
- [25] Talebitooti, R., Zarastvand, M., and Rouhani, A.H., "Investigating Hyperbolic Shear Deformation Theory on vibroacoustic Behavior of the Infinite Functionally Graded Thick Plate", *Latin American Journal of Solids and Structures*, Vol. 16, No. 1, (2019).
- [26] Talebitooti, R., Zarastvand, M., and Darvishgohari, H., "Multi-objective Optimization Approach on Diffuse Sound Transmission through Poroelastic Composite Sandwich Structure", *Journal of Sandwich Structures & Materials*, Jun 12:1099636219854748, (2019).
- [27] Motaharifar, F., Ghassabi, M., and Talebitooti, R., "Vibroacoustic Behavior of a Plate Surrounded by a Cavity Containing an Inclined Part-through Surface Crack with Arbitrary Position", *Journal of Vibration and Control*, Jun 18:1077546319853666, (2019).
- [28] Uğurlu, B., A., Kutlu, A., Ergin, and Omurtag, M. H., "Dynamics of a Rectangular Plate Resting on an Elastic Foundation and Partially in Contact with a Quiescent Fluid", *Journal of Sound and Vibration*, Vol. 317, pp. 308-328, (2008).
- [29] Kerboua, Y., Lakis, A. A., Thomas, M. and Marcouiller, L. "Vibration Analysis of Rectangular Plates Coupled with Fluid", *Applied Mathematical Modelling*, Vol. 32, pp. 2570-2586, (2008).
- [30] Cho, Seung, D., Kim, B.H., Vladimir, N., and Choi, T.M., "Natural Vibration Analysis of Rectangular Bottom Plate Structures in Contact with Fluid", *Ocean Engineering*. Vol. 103, pp. 171-179, (2015).
- [31] Khorshid, K., and Farhadi, S, "Free Vibration Analysis of a Laminated Composite Rectangular Plate in Contact with a Bounded Fluid", *Composite Structures*, Vol. 104, pp. 176-186, (2013).
- [32] Ergin, A., and B. Uğurlu. "Linear Vibration Analysis of Cantilever Plates Partially Submerged in Fluid", *Journal of Fluids and Structures*, Vol. 17, pp. 927-939, (2003).
- [33] Shahbazzabar, A., and Rahbar Ranji, A., "Effects of In-plane Loads on Free Vibration of Symmetrically Cross-ply Laminated Plates Resting on Pasternak Foundation and Coupled with Fluid", *Ocean Engineering*, Vol. 115, pp. 196-209, (2016).
- [34] Khorshidi, K., and Bakhsheshy, A., "Free Vibration Analysis of a Functionally Graded Rectangular Plate in Contact with a Bounded Fluid", *Acta Mechanica*, Vol. 226, pp. 3401-3423, (2015).

- [35] Shafiee, A.A., Daneshmand, F., Askari, E., and Mahzoon, M., “Dynamic Behavior of a Functionally Graded Plate Resting on Winkler Elastic Foundation and in Contact with Fluid”, *Struct. Eng. Mech.* Vol. 50, pp. 53-71, (2014).
- [36] Hosseini-Hashemi, Sh., Karimi, M., and Rokni, H., “Natural Frequencies of Rectangular Mindlin Plates Coupled with Stationary Fluid”, *Applied Mathematical Modelling.* Vol. 36, pp. 764-778, (2012).
- [37] Shahbazzabar, A., and Rahbar Ranji, A., “Free Vibration Analysis of Functionally Graded Plates on Two-parameter Elastic Supports and in Contact with Stationary Fluid”, *Journal of Offshore Mechanics and Arctic Engineering,* Vol. 140, pp. 021302, (2018).
- [38] Yousefzadeh, Sh, Jafari, A.A., and Mohammadzadeh, A., “Effect of Hydrostatic Pressure on Vibrating Functionally Graded Circular Plate Coupled with Bounded Fluid”, *Applied Mathematical Modelling,* Vol. 60, pp. 435-446, (2018).
- [39] Chang, T.P., and Liu, M.F., “Vibration Analysis of Rectangular Composite Plates in Contact with Fluid”, Vol. 1, pp. 101-120, (2001).
- [40] Qing, W.Y., and Yang, Z., “Nonlinear Vibrations of Moving Functionally Graded Plates Containing Porosities and Contacting with Liquid: Internal Resonance”, *Nonlinear Dynamics.* Vol. 90, pp. 1461-1480, (2017).
- [41] Reddy, J.N., “*Mechanics of Laminated Composite Plates and Shells: Theory and Analysis*”, CRC Press, (2004).
- [42] Chia, C.Y., “*Nonlinear Analysis of Plates*”, McGraw-Hill International Book Company, (1980).
- [43] Nayfeh, A.H., and Mook, D.T., “*Nonlinear Oscillation*”, John Wiley & Sons, Inc, (1995).
- [44] He, J.H., “Modified Lindstedt–Poincare Methods for Some Strongly Non-linear Oscillations: Part I: Expansion of a Constant”, *International Journal of Non-Linear Mechanics.* Vol. 37, pp. 309-314, (2002).

Nomenclature

A	Extensional stiffness
B	Bending-extensional coupling stiffness
D	Bending stiffness
E_c	Modulus of elasticity of ceramic
E_m	Modulus of elasticity of metal
I	Mass inertia related term
M	Moment resultant
N	Force resultant
P	Pressure
Q	Stiffness coefficient

- Q_x Rotation about the y axes
 Q_y Rotation about the x axes
 u_0 Displacements of any point on the middle surface of the plate in the x direction
 v_0 Displacements of any point on the middle surface of the plate in the y direction
 w_0 Displacements of any point on the middle surface of the plate in the z direction

Greek Symbols

- ρ_c Density of ceramic
 ρ_m Density of metal
 Φ Velocity potential function
 ε Normal strain
 γ Shear strain
 τ Shear stress
 σ Normal stress
 ν Poisson's ratio
 μ Plane wave number
 ϵ Book keeping parameter
 ω_L Linear natural frequency
 ω_{NL} Nonlinear natural frequency

Appendix A

$$\begin{aligned}
 C_{11} &= \frac{4C_{mn}}{9mn\pi^2} \left(\left(\frac{m\pi}{a} \right) \left(\frac{n\pi}{b} \right)^2 (A_{12} - A_{66}) - 2A_{11} \left(\frac{m\pi}{a} \right)^3 \right), \\
 C_{12} &= A_{11} \left(\frac{m\pi}{a} \right)^2 + A_{66} \left(\frac{n\pi}{b} \right)^2, & C_{13} &= \left(\frac{m\pi}{a} \right) \left(\frac{n\pi}{b} \right) (A_{12} + A_{66}) \\
 C_{14} &= B_{11} \left(\frac{m\pi}{a} \right)^2 + B_{66} \left(\frac{n\pi}{b} \right)^2, & C_{15} &= \left(\frac{m\pi}{a} \right) \left(\frac{n\pi}{b} \right) (B_{12} + B_{66}) \\
 C_{21} &= \frac{4C_{mn}}{9mn\pi^2} \left(\left(\frac{m\pi}{a} \right)^2 \left(\frac{n\pi}{b} \right) (A_{12} - A_{66}) - 2A_{22} \left(\frac{n\pi}{b} \right)^3 \right), \\
 C_{22} &= \left(\frac{m\pi}{a} \right) \left(\frac{n\pi}{b} \right) (A_{12} + A_{66}) \\
 C_{23} &= A_{66} \left(\frac{m\pi}{a} \right)^2 + A_{22} \left(\frac{n\pi}{b} \right)^2, & C_{24} &= \left(\frac{m\pi}{a} \right) \left(\frac{n\pi}{b} \right) (B_{12} + B_{66}), \\
 C_{25} &= B_{66} \left(\frac{m\pi}{a} \right)^2 + B_{22} \left(\frac{n\pi}{b} \right)^2
 \end{aligned}$$

$$\begin{aligned}
 C_{31} &= \frac{9}{32} \left(A_{11} \left(\frac{m\pi}{a} \right)^4 + A_{22} \left(\frac{n\pi}{b} \right)^4 \right) + \frac{1}{16} \left(\left(\frac{m\pi}{a} \right)^2 \left(\frac{n\pi}{b} \right)^2 (A_{12} + 2A_{66}) \right), \\
 C_{32} &= K \left(A_{55} \left(\frac{m\pi}{a} \right)^2 + A_{44} \left(\frac{n\pi}{b} \right)^2 \right) \\
 C_{33} &= KA_{55} \left(\frac{m\pi}{a} \right), \quad C_{34} = KA_{44} \left(\frac{n\pi}{b} \right), \\
 C_{35} &= \frac{8C_{mn}}{9mn\pi^2} \left(\left(\frac{n\pi}{b} \right)^2 \left(\frac{m\pi}{a} \right) (A_{12} - A_{66}) + A_{11} \left(\frac{m\pi}{a} \right)^3 \right) \\
 C_{36} &= \frac{8C_{mn}}{9mn\pi^2} \left(\left(\frac{m\pi}{a} \right)^2 \left(\frac{n\pi}{b} \right) (A_{12} - A_{66}) + A_{22} \left(\frac{n\pi}{b} \right)^3 \right), \\
 C_{37} &= \frac{8C_{mn}}{9mn\pi^2} \left(\left(\frac{n\pi}{b} \right)^2 \left(\frac{m\pi}{a} \right) (B_{12} - B_{66}) + B_{11} \left(\frac{m\pi}{a} \right)^3 \right) \\
 C_{38} &= \frac{8C_{mn}}{9mn\pi^2} \left(\left(\frac{m\pi}{a} \right)^2 \left(\frac{n\pi}{b} \right) (B_{12} - B_{66}) + B_{22} \left(\frac{n\pi}{b} \right)^3 \right), \\
 C_{41} &= \frac{4C_{mn}}{9mn\pi^2} \left(\left(\frac{n\pi}{b} \right)^2 \left(\frac{m\pi}{a} \right) (B_{12} - B_{66}) - 2B_{11} \left(\frac{m\pi}{a} \right)^3 \right) \\
 C_{42} &= KA_{55} \left(\frac{m\pi}{a} \right), \quad C_{43} = B_{11} \left(\frac{m\pi}{a} \right)^2 + B_{66} \left(\frac{n\pi}{b} \right)^2, \\
 C_{44} &= \left(\frac{m\pi}{a} \right) \left(\frac{n\pi}{b} \right) (B_{12} + B_{66}) \\
 C_{45} &= D_{11} \left(\frac{m\pi}{a} \right)^2 + D_{66} \left(\frac{n\pi}{b} \right)^2 + KA_{55}, \quad C_{46} = \left(\frac{m\pi}{a} \right) \left(\frac{n\pi}{b} \right) (D_{12} + D_{66}) \\
 C_{51} &= \frac{4C_{mn}}{9mn\pi^2} \left(\left(\frac{m\pi}{a} \right)^2 \left(\frac{n\pi}{b} \right) (B_{12} - B_{66}) - 2B_{22} \left(\frac{n\pi}{b} \right)^3 \right), \quad C_{52} = KA_{44} \left(\frac{n\pi}{b} \right), \\
 C_{53} &= \left(\frac{m\pi}{a} \right) \left(\frac{n\pi}{b} \right) (B_{12} + B_{66}) \\
 C_{54} &= B_{66} \left(\frac{m\pi}{a} \right)^2 + B_{22} \left(\frac{n\pi}{b} \right)^2, \quad C_{55} = \left(\frac{m\pi}{a} \right) \left(\frac{n\pi}{b} \right) (D_{12} + D_{66}), \\
 C_{56} &= D_{66} \left(\frac{m\pi}{a} \right)^2 + D_{22} \left(\frac{n\pi}{b} \right)^2 + KA_{44} \\
 C_{mn} &= (1 - (-1)^m)(1 - (-1)^n), \quad m = n = 1
 \end{aligned}$$

Appendix B

$$\begin{aligned}
 \alpha &= \left(\sqrt{\frac{\rho_m}{E_m}} h \right) \left(\frac{C_{32} - C_{33}C_{42}T_{33} - C_{33}C_{52}T_{34} - C_{34}C_{42}T_{43} - C_{34}C_{52}T_{44}}{I_0} \right) \\
 \beta &= \left(\sqrt{\frac{\rho_m}{E_m}} h^2 \right) (C_{35}C_{42}T_{13} + C_{35}C_{52}T_{14} + C_{36}C_{42}T_{23} + C_{36}C_{52}T_{24} + C_{11}C_{33}T_{31} \\
 &\quad + C_{21}C_{33}T_{32} + C_{33}C_{41}T_{33} + C_{37}C_{42}T_{33} + C_{33}C_{51}T_{34} + C_{37}C_{52}T_{34} \\
 &\quad + C_{11}C_{34}T_{41} + C_{21}C_{34}T_{42} + C_{34}C_{41}T_{43} + C_{38}C_{42}T_{43} + C_{34}C_{51}T_{44} \\
 &\quad + C_{38}C_{52}T_{44})/I_0
 \end{aligned}$$

$$\gamma = \left(\sqrt{\frac{\rho_m}{E_m}} h^3 \right) (C_{31} - C_{21}C_{35}T_{12} - C_{35}C_{41}T_{13} - C_{35}C_{51}T_{14} - C_{11}C_{36}T_{21} - C_{21}C_{36}T_{22} \\ - C_{36}C_{41}T_{23} - C_{36}C_{51}T_{24} - C_{11}C_{37}T_{31} - C_{21}C_{37}T_{32} - C_{37}C_{41}T_{33} \\ - C_{37}C_{51}T_{34} - C_{11}C_{38}T_{41} - C_{21}C_{38}T_{42} - C_{38}C_{41}T_{43} - C_{38}C_{51}T_{44} \\ - C_{11}C_{35}T_{11}) / I_0$$

$$T_{11} = (-C_{25}C_{45}C_{54} + C_{24}C_{46}C_{54} + C_{25}C_{44}C_{55} - C_{23}C_{46}C_{55} - C_{24}C_{44}C_{56} + C_{23}C_{45}C_{56})/G$$

$$T_{12} = (C_{15}C_{45}C_{54} - C_{14}C_{46}C_{54} - C_{15}C_{44}C_{55} + C_{13}C_{46}C_{55} + C_{14}C_{44}C_{56} - C_{13}C_{45}C_{56})/G$$

$$T_{13} = (-C_{15}C_{24}C_{54} + C_{14}C_{25}C_{54} + C_{15}C_{23}C_{55} - C_{13}C_{25}C_{55} - C_{14}C_{23}C_{56} + C_{13}C_{24}C_{56})/G$$

$$T_{14} = (C_{15}C_{24}C_{44} - C_{14}C_{25}C_{44} - C_{15}C_{23}C_{45} + C_{13}C_{25}C_{45} + C_{14}C_{23}C_{46} - C_{13}C_{24}C_{46})/G$$

$$T_{21} = (C_{25}C_{45}C_{53} - C_{24}C_{46}C_{53} - C_{25}C_{43}C_{55} + C_{22}C_{46}C_{55} + C_{24}C_{43}C_{56} - C_{22}C_{45}C_{56})/G$$

$$T_{22} = (-C_{15}C_{45}C_{53} + C_{14}C_{46}C_{53} + C_{15}C_{43}C_{55} - C_{12}C_{46}C_{55} - C_{14}C_{43}C_{56} + C_{12}C_{45}C_{56})/G$$

$$T_{23} = (C_{15}C_{24}C_{53} - C_{14}C_{25}C_{53} - C_{15}C_{22}C_{55} + C_{12}C_{25}C_{55} + C_{14}C_{22}C_{56} - C_{12}C_{24}C_{56})/G$$

$$T_{24} = (-C_{15}C_{24}C_{43} + C_{14}C_{25}C_{43} + C_{15}C_{22}C_{45} - C_{12}C_{25}C_{45} - C_{14}C_{22}C_{46} + C_{12}C_{24}C_{46})/G$$

$$T_{31} = (-C_{25}C_{44}C_{53} + C_{23}C_{46}C_{53} + C_{25}C_{43}C_{54} - C_{22}C_{46}C_{54} - C_{23}C_{43}C_{56} + C_{22}C_{44}C_{56})/G$$

$$T_{32} = (C_{15}C_{44}C_{53} - C_{13}C_{46}C_{53} - C_{15}C_{43}C_{54} + C_{12}C_{46}C_{54} + C_{13}C_{43}C_{56} - C_{12}C_{44}C_{56})/G$$

$$T_{33} = (-C_{15}C_{23}C_{53} + C_{13}C_{25}C_{53} + C_{15}C_{22}C_{54} - C_{12}C_{25}C_{54} - C_{13}C_{22}C_{56} + C_{12}C_{23}C_{56})/G$$

$$T_{34} = (C_{15}C_{23}C_{43} - C_{13}C_{25}C_{43} - C_{15}C_{22}C_{44} + C_{12}C_{25}C_{44} + C_{13}C_{22}C_{46} - C_{12}C_{23}C_{46})/G$$

$$T_{41} = (C_{24}C_{44}C_{53} - C_{23}C_{45}C_{53} - C_{24}C_{43}C_{54} + C_{22}C_{45}C_{54} + C_{23}C_{43}C_{55} - C_{22}C_{44}C_{55})/G$$

$$T_{42} = (-C_{14}C_{44}C_{53} + C_{13}C_{45}C_{53} + C_{14}C_{43}C_{54} - C_{12}C_{45}C_{54} - C_{13}C_{43}C_{55} + C_{12}C_{44}C_{55})/G$$

$$T_{43} = (C_{14}C_{23}C_{53} - C_{13}C_{24}C_{53} - C_{14}C_{22}C_{54} + C_{12}C_{24}C_{54} + C_{13}C_{22}C_{55} - C_{12}C_{23}C_{55})/G$$

$$T_{44} = (-C_{14}C_{23}C_{43} + C_{13}C_{24}C_{43} + C_{14}C_{22}C_{44} - C_{12}C_{24}C_{44} - C_{13}C_{22}C_{45} + C_{12}C_{23}C_{45})/G$$

$$G = (C_{15}C_{24}C_{44}C_{53} - C_{14}C_{25}C_{44}C_{53} - C_{15}C_{23}C_{45}C_{53} + C_{13}C_{25}C_{45}C_{53} + C_{14}C_{23}C_{46}C_{53} \\ - C_{13}C_{24}C_{46}C_{53} - C_{15}C_{24}C_{43}C_{54} + C_{14}C_{25}C_{43}C_{54} + C_{15}C_{22}C_{45}C_{54} \\ + C_{15}C_{23}C_{43}C_{55} - C_{13}C_{25}C_{43}C_{55} - C_{15}C_{22}C_{44}C_{55} + C_{12}C_{25}C_{44}C_{55} \\ + C_{13}C_{22}C_{46}C_{55} - C_{12}C_{23}C_{46}C_{55} - C_{14}C_{23}C_{43}C_{56} + C_{13}C_{24}C_{43}C_{56} \\ + C_{14}C_{22}C_{44}C_{56} - C_{12}C_{24}C_{44}C_{56} - C_{13}C_{22}C_{45}C_{56} + C_{12}C_{23}C_{45}C_{56})$$